Statins reduce intratumor cholesterol affecting adrenocortical cancer growth

Statins reduce intratumor cholesterol affecting adrenocortical cancer growth

Francesca Trotta[1]*, Paola Avena[1]*, Adele Chimento[1]*, Vittoria Rago[1], Arianna De Luca[1], Sara Sculco[1], Marta C. Nocito[1], Rocco Malivindi[1], Francesco Fallo[2], Raffaele Pezzani[2], Catia Pilon[2], Francesco M. Lasorsa[3], Simona N. Barile[3], Luigi Palmieri[3], Antonio M. Lerario[4], Vincenzo Pezzi[1**], Ivan Casaburi[1#], Rosa Sirianni[1# **]

[1]Department of Pharmacy, Health and Nutritional Sciences, University of Calabria, Arcavacata di Rende, Cosenza, Italy.
[2]Department of Medical and Surgical Sciences, University of Padua, Via Ospedale 105, 35128 Padua, Italy.
[3]Department of Biosciences, Biotechnologies and Biopharmaceutics, University of Bari, and CNR Institute of Biomembranes, Bioenergetics and Molecular Biotechnologies Bari, Italy
[4]Departments of Molecular & Integrative Physiology and Internal Medicine, University of Michigan, Medical School, Ann Arbor, MI, USA.

*Contributed equally

#Co-senior authors

**Co-corresponding

Rosa Sirianni, PhD
Dept. of Pharmacy, Health and Nutritional Sciences, University of Calabria,
Arcavacata di Rende (CS),
87036 Italy.
Phone: +39 0984 493182
Fax: +39 0984 493157

Vincenzo Pezzi, PhD
Dept. of Pharmacy, Health and Nutritional Sciences, University of Calabria,
Arcavacata di Rende (CS),
87036 Italy.
Phone: +39 0984 493148
Fax: +39 0984 493157

Short title: Statins reduce ACC growth

Abbreviations

ACC: adrenocortical cancer;
HMGCR: 3-Hydroxy-3-Methylglutaryl-CoA Reductase
ERα: estrogen receptor alpha,

40 COXIV: cytochrome c oxidase
41 OCR: oxygen consumption rate
42
43 The authors declare no potential conflicts of interest.

Abstract

Mitotane causes hypercholesterolemia in ACC patients. We suppose that cholesterol increases within the tumor and can be used to activate proliferative pathways. In this study, we used statins to decrease intratumor cholesterol and investigated the effects on ACC growth related to ERα action at the nuclear and mitochondrial levels. We first used microarray to investigate mitotane effect on genes involved in cholesterol homeostasis and evaluated their relationship with patients' survival in ACC TCGA. We then blocked cholesterol synthesis with simvastatin and determined the effects on H295R cell proliferation, estradiol production and ERα activity in vitro and in xenograft tumors. We found that mitotane increases intratumor cholesterol content and expression of genes involved in cholesterol homeostasis, among them INSIG, whose expression affects patients' survival. Treatment of H295R cells with simvastatin to block cholesterol synthesis decreased cellular cholesterol content and this affected cell viability. Simvastatin reduced estradiol production and decreased nuclear and mitochondrial ERα function. A mitochondrial target of ERα, the respiratory complex IV (COX IV) was reduced after simvastatin treatment, which profoundly affected mitochondrial respiration activating apoptosis. In vivo experiments confirmed the ability of simvastatin to reduce tumor volume and weight of grafted H295R cells, intratumor cholesterol content, Ki-67 and ERα, COX IV expression and activity and increase TUNEL positive cells. Collectively these data demonstrate that a reduction in intratumor cholesterol content prevents estradiol production, inhibits mitochondrial respiratory chain inducing apoptosis in ACC cells. Inhibition of mitochondrial respiration by simvastatin represents a novel strategy to counteract ACC growth.

Introduction

Adrenocortical carcinoma (ACC) is a rare but aggressive cancer with a very poor prognosis. At present the only valuable option for ACC therapy is an early prognosis followed by surgical resection of the tumor. Mitotane (1,1-dichloro-2-(ochlorophenyl)-2-(p-chloro-phenyl)-ethane or o,p-DDD), an inhibitor of steroid synthesis with adrenolytic activity, alone or combined with cytotoxic drugs such as etoposide, doxorubicin, and platinum agents, is the only specific treatment for ACC (1). Overall survival rate at 5-years is 16-38%, but in the case of metastatic disease (stage IV), survival rate at 5 years drops to less than 10 % (2). Because mitotane treatment has a relatively low response rate and carries significant systemic toxicity, better treatment methods are critically needed for more effective targeting and inhibition of ACC.

Mitotane works by inhibiting cytochrome P450s involved in steroid synthesis and by inhibiting SOAT1, an enzyme involved in cholesterol esterification, leading to an increase in free cholesterol toxic to the cell. Mitotane serum concentrations above 14 mg/l are required for its therapeutic effects (3). However, even with administration of high doses, effective mitotane serum concentrations are achieved in only half of patients and are never reached in others (4). Doses below 14 mg/l are less effective in inhibiting SOAT1, but still able to induce 3-hydroxy-3-methylglutaryl-coenzyme A reductase (HMGCR) activity in the liver (5), favoring an increase in serum cholesterol levels, a side effect that ACC patients experience during mitotane treatment (6). Possibly, the increase in serum cholesterol will allow the adrenal tumor to have a higher uptake. Alternatively, a direct effect of mitotane on adrenal HMGCR, impacting de novo synthesis, cannot be excluded, since the adrenal can synthesize cholesterol in the endoplasmic reticulum (7). Both uptake or de novo synthesis will increase cholesterol availability within the tumor cells, favoring activation of proliferative mechanisms.

Our previous studies have demonstrated that ACC is characterized by aromatase over-expression (8) and insulin-like growth factor II (IGF-II) (resulting overexpressed in 90% of ACCs and activating an autocrine mitogenic effect) can induce aromatase transcription (9). Then, it is possible that in ACC patients, despite normal circulating estrogen levels, a higher local estrogen production can occur, allowing estrogens, through estrogen receptor α (ERα), to foster ACC progression.

A study performed on 152 ACC patients showed that increased intra-abdominal fat is associated with tumor worsening and decreased survival (10). The rise in fat deposition observed in mitotane-treated patients can also be responsible for increased estradiol production, since the adipose tissue has high aromatase expression, which can convert steroid precursors into estrogens (11). Importantly, it has been recently suggested that adipose tissue may contain the steroidogenic machinery necessary for the initiation of de novo steroid biosynthesis from cholesterol (12). The

increase in cholesterol and body fat is also responsible for lowering hematic mitotane concentration, since the drug is a lipophilic compound and accumulates into circulating lipoprotein fractions and high-lipid-containing tissues (13).

A drug capable of reducing cholesterol synthesis both at hepatic and intratumor level would be effective in preventing ACC growth. In this study we propose statins, drugs that target HMGCR, largely used to reduce hypercholesterolemia, as a valid treatment for ACC. By reducing cholesterol synthesis within the tumor cells, statins could be a reliable mean to prevent estrogen production and then action through ERα in ACC.

Materials and Methods

Detailed experimental information is provided in the Supplemental Experimental Procedures.

Cell cultures and tissue

H295R, SW13 and Y1 cells were purchased from ATCC. H295R were cultured as previously described (14). SW13 were maintained in DMEM/F-12 with 10% fetal bovine serum (FBS). Y1 cells were maintained in DMEM/F-12 with 2.5% FBS and 15% horse serum. Cell monolayers were subcultured into 6 well plates for protein and RNA extraction (4 x 10^6 cells/plate) and 12 multi-well for colony formation assay (1x 10^3 cells/well) and grown for 14 days. Cells were treated with statins or mitotane (Sigma) in DMEM/F-12 containing 10% FBS.

Fresh-frozen samples of adrenocortical tumors, removed at surgery, were collected at the hospital-based Divisions of the University of Padua (Italy). Tissue samples were obtained with the approval of local ethics committees and written informed consent from patients. Studies were conducted in accordance with the Declaration of Helsinki guidelines as revised in 1983 and approved by the institutional review board of the University of Padua. Diagnosis of malignancy was performed according to the histopathological criteria proposed by Weiss *et al.* (15) and the modification proposed by Aubert *et al.* (16). Patients included in the mitotane-treated group received the drug for at least 4 months at the dose of 4-6 g/day.

MTT assay

The effect of simvastatin on cell viability was measured using 3-[4,5-dimethylthiazol-2-yl]-2,5-diphenyltetrazoliumbromide (MTT) assay as previously described (17). Briefly, cells were cultured in complete medium in 48 well plates (1×10^4 cells/well) for 48 h, then treated in 10% FBS medium for 24, 48 or 72 h. Fresh MTT (Sigma), resuspended in PBS, was then added to each well (final concentration 0.33 mg/mL). After 2h incubation, cells were lysed with 200 µl of DMSO and optical density was measured at 570 nm in a multi plate reader (Synergy H1, BioTek, Agilent).

Intracellular cholesterol extraction and colorimetric cholesterol assay

Cholesterol was measured using a colorimetric cholesterol assay kit (Cell Biolabs). Intracellular cholesterol was extracted from cells using a mixture of chloroform, isopropanol and NP-40 (7: 11: 0.1). The same mix was added to tumor samples of known weight, and lysed using stainless steel beads in the Bullet Blender Tissue Homogenizer (Next Advance, Inc.; Troy, NY USA). Purified water was then added to lysed samples, and upon centrifugation, the organic, bottom phase was taken and dried by vacuum centrifugation. The resulting lipid pellet was resuspended in 200 µl of

1X cholesterol assay buffer. Then, 50 µL of sample were processed according to manufacturer's instruction.

ELISA for Estradiol

The H295R cells were kept in complete medium for 48h in multi-wells of 12 ($1x10^5$ cells/well) and treated in DMEM F-12 enriched with 5% DCC-FBS (FBS treated with Dextran coated in order to repair steroids) with increasing doses of simvastatin (2.5-5-10 µM). After 48 hours of treatment the contents of 17β-estradiol (E2) was measured by means of ELISA (enzyme-linked immuno-absorbent assay) (NovaTec) following manufacturer's instruction.

Spheroids culture

A single cell suspension was prepared using enzymatic (1X Trypsin-EDTA, Sigma Aldrich, #T3924), and manual disaggregation (25 gauge needle) (18). Cells were plated at a density of 500 cells/cm^2 in spheroids medium (DMEM-F12/B27/EGF (20ng/ml)/ Pen-Strep) in non-adherent conditions, in culture dishes coated with (2-hydroxyethylmethacrylate) (poly-HEMA, Sigma, #P3932). Cells were grown for 5 days and maintained in a humidified incubator at 37°C at an atmospheric pressure in 5% (v/v) carbon dioxide/air. After 5 days of culture, spheres >50 µm were counted using an eye piece graticule, and the percentage of cells plated which formed spheres was calculated and is referred to as percentage spheroids formation, and was normalized to one (1 = 100% TSFE, tumor-spheres formation efficiency). Cells were directly seeded on low-attachment plates in the presence of treatments.

Colony formation

The NCI-H295R cells were plated in 12-well plates ($1x10^3$) and allowed to attach. Treatment commenced for 24 hours with drug alone. Untreated or simvastatin-treated cells were controls. The medium was changed and surviving cells were allowed to grow colonies of ≥50 cells for 2 weeks, washed, fixed, and stained with Coomassie blue, and counted. Total colony numbers were normalized to untreated controls.

Protein extraction and Western-blotting

H295R cells were cultured in complete medium for 48 hours in 100 mm plates ($2x10^6$ cells) before being treated in complete medium with simvastatin for 48 hours and then used for cytosolic and mitochondrial protein extraction. The extracts were then analyzed by western blotting (WB).

Total proteins were prepared using RIPA buffer. Equal amounts of proteins were subjected to WB analysis. Blots were incubated overnight at 4 °C with primary antibodies. Membranes were incubated with horseradish peroxidase (HRP)-conjugated secondary antibodies (Amersham) and immunoreactive bands were visualized with the ECL (Amersham).

Xenograft experiments

All animal procedures approved by the Ethics Research Committee University animals from Calabria (protocol No. 1077/2016-PR from the Ministry of Health to Dr. Sirianni) were performed in female Foxn1nu mice (Harlen Envigo) mice. Following H295R xenograft establishment, mice received 4 mg/kg/d of simvastatin in the water for 24 days, and tumors were harvested and weighed. The water with the treatment has been replaced every week. The dose was chosen to equal the therapeutic dose used for patients of 20 mg/d (based on the equivalence of body surface area) (19).

Immunohistochemistry

IHC experiments were performed using 8 mm thick paraffin-embedded sections of H295R xenograft tumors from mice treated with vehicle or simvastatin. Slides were deparaffinized and dehydrated and incubated over-night at 4°C with Aromatase (MBL International Corporation, Woburn, MA, USA, MCA2077S, 1:50), COXIV (Abcam, ab14744, 1:200), Ki-67 (DAKO, M7240, 1:100), CCNE (Bethyl, IHC-00341, 1:100), ERα (Santa Cruz, sc-8002, 1:50), TOM20 (Santa Cruz, sc-17764, 1:100) primary antibodies. Then, a horse biotinylated anti-mouse/rabbit IgG was applied for 1h at RT, to form the avidin biotin horseradish peroxidase complex (Vector Laboratories). Immunoreactivity was visualized by DAB (Vector Laboratories). For ERα detection was used a FITC-conjugated secondary antibodies (Santa Cruz) for 1h at RT. Fluorescent images were collected on Olympus fluorescent microscope.

Oil red O staining

H295R cells ($1x10^6$) were plated on glass coverslips for 48h and then treated for 48h with simvastatin (10 μM). The cells were washed with cold phosphate-buffered saline (PBS) and fixed with 4% paraformaldehyde for 30 min at RT. Then, the cells were stained with 0.5% Oil Red O (Sigma-Aldrich, St. Louis, MO, USA) solution for 20 min at RT and counterstained with hematoxylin for 2 min, followed by PBS washes and microscopic evaluation.

Cytochrome C oxidase (COX)/complex IV activity

Cryostat sections (8 μm) were prepared and stored at -80°C until use. For the COX activity staining, frozen sections were brought to RT, washed for 5 min with 25 mM sodium phosphate buffer, pH 7.4, and then incubated for 0.5, 1 or 2 h at 37°C with the COX incubation mixture. The COX solution consisted of 10 mg Cytochrome C (cat# C7752, Sigma-Aldrich), 10 mg 3,3'-diaminobenzidine tetrahydrochloride hydrate (cat# D5637, Sigma-Aldrich) and 2 mg catalase (cat# C1345, Sigma-Aldrich) dissolved in 10 ml of 25 mM sodium phosphate buffer. The solution was filtered after preparation and the pH was adjusted to 7.2-7.4 with 1 N NaOH.

HMGCR activity assay

The HMGCR activity in H295R lysates was measured with HMGCR Activity Assay Kit (CS1090, Sigma, USA) according to manufacturer's instructions. The assay is based on the spectrophotometric measurement of the decrease in absorbance at 340 nm, which represents the oxidation of NADPH by the catalytic subunit of HMGCR in the presence of the substrate HMG-CoA. Cells were lysed in RIPA buffer containing protease inhibitors. Two microliters of cell lysate were used to measure HMGCR activity. One unit converts 1.0 μmol of NADPH to NADP+ per 1 min at 37°C. The unit specific activity is defined as μmol/min/mg protein (units/mg P).

Detection of apoptosis by TUNEL assay

The induction of apoptosis was assessed by the TUNEL assay (Terminal deoxynucleotidyl transferase dUTP Nick End Labeling), a method that evaluates the fragmentation of DNA. The click-it® TUNEL Alexa Fluor® Imaging Assay kit (Invitrogen) was used, following the manufacturer's instructions. Sections of vehicle- and simvastatin-treated tumors from paraffin-embedded H295R xenografts were cut to a thickness of 5 μm, deparaffinized and dehydrated and then used for the assay.

Seahorse XFe96 metabolic flux analysis

Real-time oxygen consumption rates (OCR) for H295R cells treated with simvastatin or vehicle (control) were determined using the Seahorse Extracellular Flux (XF96) analyzer (Seahorse Bioscience, MA, USA). H295R cells were maintained in DMEM supplemented with 10% fetal bovine serum (FBS), 2 mM GlutaMAX, and 1% Pen/Strep. $7x10^4$ cells were seeded per well into XF96-well cell culture plates (Seahorse Bioscience, MA, USA), and incubated overnight at 37°C in a 5% CO2 humidified atmosphere. After 24h, cells were treated with simvastatin (2.5, 5 and 10 μM) for 48h. At the end of treatment, cells were processed as previously published (20).

253 **Microarray**

254 H295R cells ($1x10^5$) were plated on 60 mm dishes for 48h and then treated for 24h with Mitotane
255 (25 μM). RNA was extracted using PureLink™ RNA Mini Kit (Thermo Fisher). The quality of total
256 RNA was first assessed using an Agilent Bioanalyzer 2100 (Agilent Technologies, Palo Alto, CA).
257 Biotin-labeled cDNA targets were synthesized starting from 150 ng of total RNA. Double stranded
258 cDNA synthesis and related cRNA was performed with GeneChip® WT Plus Kit (Affymetrix,
259 Santa Clara, CA). With the same kit was synthesized the sense strand cDNA before to be
260 fragmented and labeled. All steps of the labeling protocol were performed as suggested by
261 Affymetrix, starting from 5.5 ug of ssDNA. Hybridization was performed using the GeneChip®
262 Hybridization, Wash and Stain Kit. A single GeneChip® Clariom S was then hybridized with each
263 biotin-labeled sense target. GeneChip arrays were scanned using an Affymetrix GeneChip®
264 Scanner 3000 7G using default parameters. Affymetrix GeneChip® Command Console software
265 (AGCC) was used to acquire GeneChip® images and generate .DAT and CEL files, which were
266 used for subsequent analysis with proprietary software.
267
268 **RNA extraction, reverse transcription and real time PCR**
269 Following total RNA extraction, 1 μg of total RNA was reverse transcribed and then used for PCR
270 reactions were performed in the iCycler iQ Detection System (Bio-Rad Laboratories S.r.l., Milano,
271 Italia). Final results were expressed as n-fold differences in gene expression relative to 18S and
272 calibrator, calculated using the ΔΔCt method as previously shown (14).
273
274 **Patients' data analysis**
275 Gene expression and survival data were obtained using two independent cohorts of adrenocortical
276 tumors were used: Expression Cohort included 33 ACC, 22 ACA (adrenocortical adenoma) and 10
277 NA (normal adrenal) (GEO dataset GSE33371) and TCGA cohort included 78 ACC
278 (https://portal.gdc.cancer.gov/legacy-archive).
279
280 **Statistics**
281 All experiments were performed at least three times. Data were expressed as mean values +
282 standard error), statistical significance between control and treated samples was analyzed using
283 GraphPad Prism 5.0 (GraphPad Software, Inc.; La Jolla, CA) software. Control and treated groups
284 were compared using t-test or the analysis of variance (ANOVA). Significance was defined as $p <$
285 0.05. Microarray data analysis was performed using Partek Genomics Suite software (PGS), version
286 6.6 (6.16.0812 for Mac). Affymetrix CEL-files were extracted, normalized and summarized using

RMA algorithm (CEL file imported by Partek on Wed Feb 21 10:25:17 2018; Probes to Import: Interrogating Probes; Probe filtering: skip; Algorithm: RMA; Background Correction: RMA Background Correction; Normalization: Quantile Normalization; Log Probes using Base: 2; Probeset Summarization: Median Polish) (21-23). Genes differentially expressed were identified using a t-test.

Results

Mitotane increases intratumor cholesterol content by affecting expression of genes involved in the regulation of cholesterol homeostasis.

Here we wanted to determine if mitotane can also increase cholesterol content in the tumor. As it can be seen in **Fig. 1A**, cholesterol is increased in ACC from patients treated with mitotane compared to tumors from ACC patients that underwent surgery prior to any treatment. A key enzyme in cholesterol synthesis is HMGCoA reductase (HMGCR). We conducted a retrospective analysis of publicly available microarray data from ACC patients' cohorts. Expression levels of HMGCR are higher in ACC when compared to the normal adrenal (NC) (**Fig. 1B**). However, its expression does not affect patients' survival (**Fig. 1C**). We evaluated HMGCR protein expression and activity in H295R cells after 2 and 14 days of mitotane treatment. As previously demonstrated in hepatocytes, mitotane increases the enzyme activity (**Fig. 1D**).

We also used H295R cells treated with mitotane for 24 hours to perform gene expression microarray analysis. Using as cutoff of 1.5 in fold change and a p value ≤ 0.05 we identified 344 transcripts regulated by mitotane. Importantly, an enrichment analysis for the categories of Gene Ontology (GO), indicated that the drug preferentially increases expression of genes involved in metabolism, and more specifically we looked into cholesterol metabolism (**Fig. 1E**). Among the genes present in this GO group we further investigated sterol regulatory element-binding protein 1 (SREBP1) and Insulin induced gene 1 (INSIG1) encoding for proteins working as cholesterol sensors, and ATP-binding cassette sub-family G member 1 (ABCG1), encoding for a protein that mediates cholesterol efflux from the cells to ApoA1 (apolipoprotein A1), a component of HDL. Results from microarray were confirmed by real-time PCR using short-term (24h) and long-term (2 weeks and 3 weeks) mitotane-treated H295R cells. As observed in microarray data, SREBP1, INSIG1, and ABCG1 expression was decreased after 24h treatment (**Fig. 1F, 1I, 1L**). On the long term treatment, expression of SREBP1 was maintained low (**Fig. 1G**). Survival data for this factor show that when its expression is low patients have a trend to a worse outcome, even if not significant (**Fig. 1H**). For INSIG1 and ABCG1 we found that long term treatment with mitotane did not produce a decrease in gene expression, but mRNA levels were kept similar to those seen in untreated samples (**Fig. 1J, 1M**). The higher expression of these genes maintained in the presence of increased cholesterol amounts (caused by mitotane) indicate loss of cell ability to sense cholesterol levels. Importantly, survival data for INSIG indicate that higher expression is associated with worse survival (**Fig. 1K**). A similar trend in the association was observed for ABCG1, even if there was not a significant difference between the two groups (**Fig. 1N**).

A decrease in ACC intracellular cholesterol positively associates with decreased tumor growth *in vitro* and *in vivo*.

The use of simvastatin was able to reduce H295R cell viability in a time and dose-dependent manner (**Fig. 2A**). Importantly, the decreased cell viability was rescued by addition of mevalonate, the product of HMGCoA reductase activity (**Fig. 2B**). These effects were reproduced by fluvastatin and rosuvastatin, (**Fig. S1A)**. Additionally, we used two additional cell lines, SW13 and Y1, and found that all tested statins produced effects similar two those observed in H295R cells (**Fig. S1 B, C**). In the clonogenic assay, simvastatin treated cells formed significantly less colonies when compared to vehicle treated cells, illustrating the tumor suppressor function of this drug (**Fig. 2C**). When H295R cells were grown as spheroids in the presence of simvastatin, we observed a substantial dose-dependent decrease in sphere numbers (**Fig. 2D**). To evaluate if intratumor cholesterol depletion could reduce ACC growth *in vivo*, xenografts were generated by implanting H295R cells in the flank of athymic nude mice. When tumors reached an average of 200 mm^3 mice were administered vehicle versus simvastatin at 4 mg/kg/day for 24 days and tumors were measured twice a week. Tumor growth of the statin treated group was significantly smaller than the vehicle treated group (**Fig. 2E**). Tumor volume at the end of the experiment was 60% smaller in animals receiving simvastatin (**Fig. 2E**), and tumor weight was decreased by 58% (**Fig. 2F**). In parallel with the decline in tumor size with simvastatin, there was a decrease in Ki-67 staining (**Fig. 2G and Fig. S2A**).

Decreased cholesterol availability in ACC impairs estradiol production

After 48h treatment simvastatin at the dose of 10 µM caused a 33% reduction in intracellular cholesterol (**Fig. 3A**). We also evaluated cholesterol content in of H295R xenografts. By adjusting to tissue weight we found a concentration of 9 ng/mg of tissue, while statin decreased this amount to 6.3 ng/mg of tissue (**Fig. 3B**). In addition, frozen sections from tumors were stained for lipids using Oil Red O, less red stain is observed in treated tumors, indicative of a reduced amount of lipid deposition (**Fig. 3B and Fig. S2B**). Thus, intratumor cholesterol has an important cell-autonomous role in ACC growth and in parallel statins lessens ACC tumor development. Treatment of H295R cells for 48h with increasing concentrations of simvastatin decreased E2 production in a dose dependent manner, as demonstrated by ELISA of H295R culture media, with 10 µM producing a 50% decrease in E2 content (**Fig. 3C**). When we evaluated aromatase (CYP19) gene expression we did not find any change in mRNA, neither in vitro (**Fig. 3D**) nor in vivo (**Fig. 3G**), indicating that simvastatin does not affect transcriptional regulation of this gene. In fact, expression of steroidogenic factor 1 (SF-1) did not change after simvastatin treatment (**Fig. 3E**). However, WB

analysis indicated a decrease in aromatase protein content following statin treatment of H295R (**Fig. 3F**), data that was confirmed by IHC on xenografts tumors (**Fig. 3H and Fig. S2C**). Additionally, the presence of mevalonate was able to overcome the inhibition on aromatase expression seen in the presence of simvastatin (**Fig. S3A**).

Decreased E2 availability in ACC impairs ERα function.

ERα has a role in regulating transcription of mitochondrial genes involved in cellular respiration (24). We evaluated both nuclear and mitochondrial ERα activity after simvastatin treatment. Expression of ERα was decreased by simvastatin in vitro (**Fig. 4A Fig. S4A and S4B**) and in vivo (**Fig. 4B Fig. S2D**), a similar effect was observed on cyclin E, a known target of ERα, both *in vitro* and *in vivo* (**Fig. 4C, D Fig. S2E**). Additionally, the presence of mevalonate was able to overcome the inhibition on ERα expression seen in the presence of simvastatin (**Fig. S3A**).

These effects are opposite to those elicited by E2, which instead increased cyclin E expression (**Fig. S3B**). Mitochondrial protein fraction was used for WB analysis of ERα, we observed that simvastatin treated samples had a lower content of the nuclear receptor (**Fig. 4E**). WB analysis of all the components of the respiratory chain (COX I to IV plus ATP synthase) can be performed using a mix of 5 different antibodies (OX-PHOS). With this approach we identified a decreased expression of COXIV (**Fig. 4F** and **S4A, S4B**), a known target of ERα. On the contrary, E2 treatment increased COXIV expression, and is able to prevent statin inhibitory effect (**Fig. S3C).** Data were also confirmed on statin-treated xenografts where we observed a reduced COXIV expression (**Fig. 4G** and **Fig. S2F**) and activity (**Fig. 4H** and **Fig. S2G**) compared to vehicle treated xenografts. We monitored cellular oxygen consumption rates (OCR), and demonstrated that simvastatin is able to reduce oxygen consumption in a dose-dependent manner (**Fig. 5A**). Statin exposure profoundly affected the oxidative metabolism of H295R cells. Indeed, 16 h of treatment induced a clear dose-dependent decrease of the basal (**Fig. 5B**) and maximal respiration (**Fig. 5C**) as well as ATP turnover (**Fig. 5E**) and spare capacity (**Fig. 5F**). No effect was observed on proton leak (**Fig. 5D**). We also used immunoblotting to monitor the abundance of a known reliable marker of mitochondrial mass, TOM20, in response to simvastatin treatment. We found that treated H295R cells displayed a reduced expression of TOM20, *in vitro* and *in vivo* (**Fig. 5G, 5H and Fig. S2H**).

Decreased cholesterol availability in ACC activates an apoptotic pathway.

BAK expression and PARP-1 cleavage, were increased in H295R cells treated for 48h with simvastatin, indicating activation of apoptosis (**Fig. 6A** and **Fig. S4C, S4D**), further confirmed by TUNEL assay (**Fig. 6B**). Similarly, evaluation of apoptosis on H295R xenografts sections revealed

an increase of TUNEL positive cells under simvastatin treatment (**Fig. 6C**). Since Bak gene is under c-Jun transcriptional control (25), we evaluated c-Jun protein levels after simvastatin treatment. After 48h we observed increased levels of c-Jun and its phosphorylation status, as well as increased levels of pERK1/2, whose sustained activation is associated with apoptosis (26). Addition of mevalonate prevented activation of these kinases in response to simvastatin (**Fig. 6D and Fig. S4C, S4D**). Specific inhibitors for ERK1/2 and JNK abrogated Jun and ERK1/2 activation/phosphorylation preventing apoptosis, as indicated by the loss of PARP1 cleavage. These data indicate ERK1/2 and JNK as part of simvastatin-induced apoptotic mechanism (**Fig. 6E**). Similarly to simvastatin, fluvastatin and rosuvastatin inhibited estrogen signaling and activated apoptosis in H295R cells (**Fig. S4E and S4F).**

Discussion

Mitotane represents the first-line therapy for patients with ACC. However, mitotane alone or combined with chemotherapy shows limited efficacy on advanced disease. In addition, mitotane has high toxicity and several side effects among which hypercholesterolemia (6,27). Data from almost 40 years ago report the ability of mitotane to increase liver HMGCR activity *in vitro* and *in vivo* (5). Since the adrenal synthesizes cholesterol *de novo*, mitotane could have a direct effect on adrenal cholesterol synthesis. Having higher cholesterol bioavailability, tumor cells can foster their own growth. To support our hypothesis, we first demonstrate an increase in intratumor cholesterol in ACC patients treated with mitotane compared to untreated patients. Using previously published microarray data publically available (28) we demonstrated the presence of increased HMGCR expression in ACC samples, which, however, was not associated with decreased survival rate. Increased intratumor cholesterol following mitotane treatment could be due to an increased activity of HMGCR rather than to an increased expression, with the former influencing survival more than the latter. Microarray analysis of mitotane-treated H295R cells helped us in identifying genes involved in cholesterol metabolism and modulated by the drug. Among them, we validated INSIG1, SREBP1 and ABCG1. INSIG1 encodes for a protein that retains a chaperone protein (SCAP) in the endoplasmic reticulum, SCAP is necessary for delivery of SREBP1 to the Golgi, where SREBP1 becomes active. SREBP1, increases transcription of cholesterol synthesizing genes among which HMGCR (29).

Short-term mitotane decreases INSIG1 and SREBP1 expression, while long term-mitotane maintains low SREBP1 but high INSIG1 expression. When looking at survival data of ACC patients, high INSIG1 is associated with a shorter survival. ABCG1 belongs to the family of ATP binding cassette and mediates cholesterol efflux (30). Its expression is decreased by short-term mitotane treatment, but this effect is lost after prolonged treatment, favoring cholesterol accumulation. Since, mitotane has a prevalent accumulation in adipose tissue, the circulating levels are often reduced (13,31), and the therapeutic concentrations of mitotane (between 14–20 μg/mL, 40-60μM) are not always reached in patients. Importantly, lower doses (10 and 25 μM) produce effects that are different from what seen using 40μM. This raises a question, could cells, in the presence of lower doses of mitotane, escape the normal control of cholesterol homeostasis? Can the increase in cholesterol be responsible for long-term adjustment to mitotane?

Several reports propose a promising role for statins in cancer treatment (32). Here we demonstrate that simvastatin can reduce intratumor cholesterol synthesis. Based on MTT assay IC50 for simvastatin was calculated to be 10 μM. Since 1 μM simvastatin in the media corresponds to the dose of 0.4586 mg/kg of body weight, we decided to treat mice with 4 mg/Kg/day. This dose is

equivalent to a human dose of 20 mg/d based on body surface area equivalency. This dose was effective in producing more that 60% decrease in tumor growth. Importantly, this dose decreased intratumor cholesterol content, supporting our hypothesis that a reduction in intratumor cholesterol can decrease ACC growth. Interest for statins is not new for the therapy of ACC, however, it has been considered in association with mitotane to reduce hypercholesterolemia (6,33). Our data instead suggest the possibility of using lipophilic statins without mitotane but eventually with cytotoxic drugs. Simvastatin, which appears to be the most effective among the tested drugs, shouldn't be combined with mitotane, which is a known inducer of CYP3A4, a member of the cytochrome P450 family involved in simvastatin metabolism. A recent case-study evaluated management of hypercholesterolemia induced by mitotane treatment. A patient was co-administered with mitotane and statins, but despite cholesterol lowering drugs, it was observed a rise for total cholesterol and LDL-c level. Importantly the patient had 2 local recurrences within a 7 year-period, however, the course of ACC in this patient's case has been better than average. This data supports our hypothesis that cholesterol can be implicated in ACC progression.

Cholesterol in tumor adrenal cells is used for steroid synthesis, and a decrease in its availability would affect estradiol production. Our previous study demonstrated that E2 increases tumor growth, and Tamoxifen, which blocks ERα activity, prevents its effects (9). With this information as background, we wanted to investigate if the reduced E2 production, seen after simvastatin treatment, could interfere with ERα function. We first observed a reduction in CCNE, a known nuclear target of ERα. Additionally, we investigated if the expression of mitochondrial targets of ERα could be influenced by simvastatin. To support a role for ERα in the mitochondria of tumor adrenal, we show that E2 treatment increases the amount of COXIV levels and prevents simvastatin inhibitory effect.

Additionally, it was reported a direct effect of statins on mitochondrial function, consequent to a deficiency of complex I (34). The novelty of our data is the involvement of ERα/complex IV in statin-mediated apoptosis. The reduction in COXIV alters the functioning of mitochondrial respiration, changing the mitochondrial potential ultimately leading to organelle damage. High COXIV activity within the tumor occurs in a significant subset of patients with high grade gliomas and is an independent predictor of poor outcome (35). Importantly, it has been postulated that COXIV activity may be required for the anchorage-independent growth of lung cancer cells (36). In general, mitochondria appear to be an appealing target for the treatment of cancer (37). Effects on COXIV negatively influence mitochondrial function as demonstrated by reduced oxygen consumption rate (OCR). We have previously demonstrated that a reduced cell growth is observed in breast cancer cells treated with XCT790, a drug that targets ERRα, a master regulator of cell

metabolism. ERRα inhibition reduces OCR and prevents tumor growth (20). We have also used XCT790 to block ERRα in ACC and demonstrated its efficacy in reducing tumor growth (38), further establishing that impairing mitochondrial function, reduces ACC growth. It has been shown that mitotane significantly impairs mitochondrial respiratory chain function by selectively inhibiting enzymatic complex IV activity. However, as a consequence of respiratory chain inhibition, mitotane causes a compensatory increase of mitochondrial biogenesis (39). Differently from mitotane, simvastatin reduces TOM20, a marker of mitochondrial mass. Reduced mitochondrial function after treatment with simvastatin causes cell death by apoptosis, the same type of cell death that is observed in H295R and SW13 cells in response to mitotane. This apoptotic mechanism requires activation of c-Jun and sustained ERK1/2 phosphorylation. Farnesyl pyrophosphate (FPP) or geranylgeranyl pyrophosphate (GGPP) are products of mevalonate that can be anchored onto intracellular proteins through prenylation, thereby ensuring the re-localization of the target proteins in the cell membranes (40-42). Ras is a prenylated protein upstream of ERK1/2 activation. The observation that ERK1/2 phosphorylation is maintained in the presence of simvastatin, evidences that its phosphorylation is independent of Ras and potentially involves different pathways. We found that ERK phosphorylation is prevented by addition of p38 and JNK inhibitors, implicating these kinases in the observed sustained ERK activation. Jun expression and activation are increased by treatment with simvastatin and are reversed by addition of mevalonate, which also prevents PARP-1 cleavage, confirming that the apoptotic mechanism is dependent on cholesterol depletion.

Collectively our data support the hypothesis of using statins for the treatment of ACC. Further preclinical studies are warranted to establish effects on tumor growth when used in combination with chemotherapy. However, their use in therapy as cholesterol lowering drugs will easily translate preclinical studies into a clinical trial.

Authors' Contributions

Conception and design: Ivan Casaburi, Vincenzo Pezzi, Rosa Sirianni

Development of methodology: Francesca Trotta, Adele Chimento, Paola Avena, Vittoria Rago, Arianna De Luca, Francesco M. Lasorsa, Simona N. Basile, Sara Sculco, Marta Nocito, Rosa Sirianni, Ivan Casaburi,

Acquisition of data (provided animals, acquired and managed patients, provided facilities, etc.): Rocco Malivindi, Francesca Trotta, Rosa Sirianni,

Analysis and interpretation of data (e.g., statistical analysis, biostatistics, computational analysis): Antonio M. Lerario, Francesco M. Lasorsa, Simona N. Basile, Luigi Palmieri, Raffaele Pezzani, Francesco Fallo, Catia Pilon, Rosa Sirianni, Ivan Casaburi,

Writing, review, and/or revision of the manuscript: Rosa Sirianni, Ivan Casaburi, Adele Chimento, Paola Avena

Administrative, technical, or material support (i.e., reporting or organizing data, constructing databases): Francesca Trotta, Arianna De Luca,

Study supervision: Ivan Casaburi, Vincenzo Pezzi, Rosa Sirianni

Acknowledgments

This work was supported by Associazione Italiana per la Ricerca sul Cancro (AIRC), grant IG15230 to Dr Rosa Sirianni and IG20122 to Dr Vincenzo Pezzi; Drs Trotta Francesca and Paola Avena were supported by a fellowship from AIRC.

References

1. Kirschner LS. The next generation of therapies for adrenocortical cancers. Trends in endocrinology and metabolism: TEM **2012**;23(7):343-50 doi 10.1016/j.tem.2012.04.001.

2. Fassnacht M, Johanssen S, Quinkler M, Bucsky P, Willenberg HS, Beuschlein F, *et al.* Limited prognostic value of the 2004 International Union Against Cancer staging classification for adrenocortical carcinoma: proposal for a Revised TNM Classification. Cancer **2009**;115(2):243-50 doi 10.1002/cncr.24030.

3. Hermsen IG, Fassnacht M, Terzolo M, Houterman S, den Hartigh J, Leboulleux S, *et al.* Plasma concentrations of o,p'DDD, o,p'DDA, and o,p'DDE as predictors of tumor response to mitotane in adrenocortical carcinoma: results of a retrospective ENS@T multicenter study. The Journal of clinical endocrinology and metabolism **2011**;96(6):1844-51 doi 10.1210/jc.2010-2676.

4. Kerkhofs TM, Baudin E, Terzolo M, Allolio B, Chadarevian R, Mueller HH, *et al.* Comparison of two mitotane starting dose regimens in patients with advanced adrenocortical carcinoma. The Journal of clinical endocrinology and metabolism **2013**;98(12):4759-67 doi 10.1210/jc.2013-2281.

5. Stacpoole PW, Varnado CE, Island DP. Stimulation of rat liver 3-hydroxy-3-methylglutaryl-coenzyme A reductase activity by o,p'-DDD. Biochemical pharmacology **1982**;31(5):857-60.

6. Maher VM, Trainer PJ, Scoppola A, Anderson JV, Thompson GR, Besser GM. Possible mechanism and treatment of o,p'DDD-induced hypercholesterolaemia. The Quarterly journal of medicine **1992**;84(305):671-9.

7. Miller WL. Steroidogenesis: Unanswered Questions. Trends in endocrinology and metabolism: TEM **2017**;28(11):771-93 doi 10.1016/j.tem.2017.09.002.

8. Barzon L, Masi G, Pacenti M, Trevisan M, Fallo F, Remo A, *et al.* Expression of aromatase and estrogen receptors in human adrenocortical tumors. Virchows Archiv : an international journal of pathology **2008**;452(2):181-91 doi 10.1007/s00428-007-0542-0.

9. Sirianni R, Zolea F, Chimento A, Ruggiero C, Cerquetti L, Fallo F, *et al.* Targeting estrogen receptor-alpha reduces adrenocortical cancer (ACC) cell growth in vitro and in vivo: potential therapeutic role of selective estrogen receptor modulators (SERMs) for ACC treatment. The Journal of clinical endocrinology and metabolism **2012**;97(12):E2238-50 doi 10.1210/jc.2012-2374.

10. Miller BS, Ignatoski KM, Daignault S, Lindland C, Doherty M, Gauger PG, *et al.* Worsening central sarcopenia and increasing intra-abdominal fat correlate with decreased survival in patients with adrenocortical carcinoma. World journal of surgery **2012**;36(7):1509-16 doi 10.1007/s00268-012-1581-5.

11. Simpson ER. Sources of estrogen and their importance. The Journal of steroid biochemistry and molecular biology **2003**;86(3-5):225-30.

12. Li J, Papadopoulos V, Vihma V. Steroid biosynthesis in adipose tissue. Steroids **2015**;103:89-104 doi 10.1016/j.steroids.2015.03.016.

13. Hescot S, Seck A, Guerin M, Cockenpot F, Huby T, Broutin S, *et al.* Lipoprotein-Free Mitotane Exerts High Cytotoxic Activity in Adrenocortical Carcinoma. The Journal of clinical endocrinology and metabolism **2015**;100(8):2890-8 doi 10.1210/JC.2015-2080.

14. Chimento A, Sirianni R, Casaburi I, Zolea F, Rizza P, Avena P, *et al.* GPER agonist G-1 decreases adrenocortical carcinoma (ACC) cell growth in vitro and in vivo. Oncotarget **2015**;6(22):19190-203 doi 10.18632/oncotarget.4241.

15. Weiss LM, Medeiros LJ, Vickery AL, Jr. Pathologic features of prognostic significance in adrenocortical carcinoma. The American journal of surgical pathology **1989**;13(3):202-6.

16. Aubert S, Wacrenier A, Leroy X, Devos P, Carnaille B, Proye C, *et al.* Weiss system revisited: a clinicopathologic and immunohistochemical study of 49 adrenocortical tumors. The American journal of surgical pathology **2002**;26(12):1612-9.

17. De Luca A, Avena P, Sirianni R, Chimento A, Fallo F, Pilon C, *et al.* Role of Scaffold Protein Proline-, Glutamic Acid-, and Leucine-Rich Protein 1 (PELP1) in the Modulation of Adrenocortical Cancer Cell Growth. Cells **2017**;6(4) doi 10.3390/cells6040042.

18. Shaw FL, Harrison H, Spence K, Ablett MP, Simões BM, Farnie G, *et al.* A Detailed Mammosphere Assay Protocol for the Quantification of Breast Stem Cell Activity. Journal of Mammary Gland Biology and Neoplasia **2012**;17(2):111-7 doi 10.1007/s10911-012-9255-3.

19. Reagan-Shaw S, Nihal M, Ahmad N. Dose translation from animal to human studies revisited. FASEB journal : official publication of the Federation of American Societies for Experimental Biology **2008**;22(3):659-61 doi 10.1096/fj.07-9574LSF.

20. De Luca A, Fiorillo M, Peiris-Pages M, Ozsvari B, Smith DL, Sanchez-Alvarez R, *et al.* Mitochondrial biogenesis is required for the anchorage-independent survival and propagation of stem-like cancer cells. Oncotarget **2015**;6(17):14777-95 doi 10.18632/oncotarget.4401.

21. Bolstad BM, Irizarry RA, Astrand M, Speed TP. A comparison of normalization methods for high density oligonucleotide array data based on variance and bias. Bioinformatics **2003**;19(2):185-93 doi 10.1093/bioinformatics/19.2.185.

22. Irizarry RA, Bolstad BM, Collin F, Cope LM, Hobbs B, Speed TP. Summaries of Affymetrix GeneChip probe level data. Nucleic acids research **2003**;31(4):e15 doi 10.1093/nar/gng015.

23. Wu ZJ, Irizarry RA, Gentleman R, Martinez-Murillo F, Spencer F. A model-based background adjustment for oligonucleotide expression arrays. Journal of the American Statistical Association **2004**;99(468):909-17 doi 10.1198/016214504000000683.

24. Chen JQ, Cammarata PR, Baines CP, Yager JD. Regulation of mitochondrial respiratory chain biogenesis by estrogens/estrogen receptors and physiological, pathological and pharmacological implications. Biochimica et biophysica acta **2009**;1793(10):1540-70 doi 10.1016/j.bbamcr.2009.06.001.

25. Jin HO, Park IC, An S, Lee HC, Woo SH, Hong YJ, *et al.* Up-regulation of Bak and Bim via JNK downstream pathway in the response to nitric oxide in human glioblastoma cells. Journal of cellular physiology **2006**;206(2):477-86 doi 10.1002/jcp.20488.

26. Cagnol S, Chambard JC. ERK and cell death: mechanisms of ERK-induced cell death--apoptosis, autophagy and senescence. The FEBS journal **2010**;277(1):2-21 doi 10.1111/j.1742-4658.2009.07366.x.

27. Daffara F, De Francia S, Reimondo G, Zaggia B, Aroasio E, Porpiglia F, *et al.* Prospective evaluation of mitotane toxicity in adrenocortical cancer patients treated adjuvantly. Endocrine-related cancer **2008**;15(4):1043-53 doi 10.1677/ERC-08-0103.

28. Barlaskar FM, Spalding AC, Heaton JH, Kuick R, Kim AC, Thomas DG, *et al.* Preclinical targeting of the type I insulin-like growth factor receptor in adrenocortical carcinoma. The Journal of clinical endocrinology and metabolism **2009**;94(1):204-12 doi 10.1210/jc.2008-1456.

29. Weber LW, Boll M, Stampfl A. Maintaining cholesterol homeostasis: sterol regulatory element-binding proteins. World journal of gastroenterology **2004**;10(21):3081-7.

30. Yvan-Charvet L, Wang N, Tall AR. Role of HDL, ABCA1, and ABCG1 transporters in cholesterol efflux and immune responses. Arteriosclerosis, thrombosis, and vascular biology **2010**;30(2):139-43 doi 10.1161/ATVBAHA.108.179283.

31. van Slooten H, Moolenaar AJ, van Seters AP, Smeenk D. The treatment of adrenocortical carcinoma with o,p'-DDD: prognostic implications of serum level monitoring. European journal of cancer & clinical oncology **1984**;20(1):47-53.

32. Zhong S, Zhang X, Chen L, Ma T, Tang J, Zhao J. Statin use and mortality in cancer patients: Systematic review and meta-analysis of observational studies. Cancer treatment reviews **2015**;41(6):554-67 doi 10.1016/j.ctrv.2015.04.005.

33. Tsakiridou ED, Liberopoulos E, Giotaki Z, Tigas S. Proprotein convertase subtilisin-kexin type 9 (PCSK9) inhibitor use in the management of resistant hypercholesterolemia induced by mitotane treatment for adrenocortical cancer. Journal of clinical lipidology **2018**;12(3):826-9 doi 10.1016/j.jacl.2018.03.078.

34. Sirvent P, Bordenave S, Vermaelen M, Roels B, Vassort G, Mercier J, *et al.* Simvastatin induces impairment in skeletal muscle while heart is protected. Biochemical and biophysical research communications **2005**;338(3):1426-34 doi 10.1016/j.bbrc.2005.10.108.

35. Griguer CE, Cantor AB, Fathallah-Shaykh HM, Gillespie GY, Gordon AS, Markert JM, *et al.* Prognostic relevance of cytochrome C oxidase in primary glioblastoma multiforme. PloS one **2013**;8(4):e61035 doi 10.1371/journal.pone.0061035.

36. Telang S, Nelson KK, Siow DL, Yalcin A, Thornburg JM, Imbert-Fernandez Y, *et al.* Cytochrome c oxidase is activated by the oncoprotein Ras and is required for A549 lung adenocarcinoma growth. Molecular cancer **2012**;11:60 doi 10.1186/1476-4598-11-60.

37. Ralph SJ, Neuzil J. Mitochondria as targets for cancer therapy. Molecular nutrition & food research **2009**;53(1):9-28 doi 10.1002/mnfr.200800044.

38. Casaburi I, Avena P, De Luca A, Chimento A, Sirianni R, Malivindi R, *et al.* Estrogen related receptor alpha (ERRalpha) a promising target for the therapy of adrenocortical carcinoma (ACC). Oncotarget **2015**;6(28):25135-48 doi 10.18632/oncotarget.4722.

39. Hescot S, Slama A, Lombes A, Paci A, Remy H, Leboulleux S, *et al.* Mitotane alters mitochondrial respiratory chain activity by inducing cytochrome c oxidase defect in human adrenocortical cells. Endocrine-related cancer **2013**;20(3):371-81 doi 10.1530/ERC-12-0368.

40. Nishida S, Matsuoka H, Tsubaki M, Tanimori Y, Yanae M, Fujii Y, *et al.* Mevastatin induces apoptosis in HL60 cells dependently on decrease in phosphorylated ERK. Molecular and cellular biochemistry **2005**;269(1-2):109-14.

41. Yanae M, Tsubaki M, Satou T, Itoh T, Imano M, Yamazoe Y, *et al.* Statin-induced apoptosis via the suppression of ERK1/2 and Akt activation by inhibition of the geranylgeranyl-pyrophosphate biosynthesis in glioblastoma. Journal of experimental & clinical cancer research : CR **2011**;30:74 doi 10.1186/1756-9966-30-74.

42. Wu J, Wong WW, Khosravi F, Minden MD, Penn LZ. Blocking the Raf/MEK/ERK pathway sensitizes acute myelogenous leukemia cells to lovastatin-induced apoptosis. Cancer research **2004**;64(18):6461-8 doi 10.1158/0008-5472.CAN-04-0866.

Figure legends

FIGURE 1. **Mitotane changes the expression of genes involved in cholesterol homeostasis in ACC and negatively affects patients' survival. A**) Cholesterol was extracted from human ACC samples and its content (ng/mg tissue) measured by colorimetric assay (- Mitotane, n=5, + Mitotane, n=7, *p<0.03). **B)** Box plot graph for HMGCR gene expression in ACA (adrenocortical adenoma), ACC (adrenocortical carcinoma) and NC (normal adrenal) human samples. ACC-ACA: p-value=0.08, ACA-NC: p-value=0.26, ACC-NC: p-value=0.26. Statistical significance was calculated using *limma*. **C**) Survival time in ACC patients according to HMGCR gene expression. **D**) HMGCR expression and activity was evaluated in H295R cells untreated (basal) or treated for 2 and 14 days with mitotane 10μM. **E**) RNA from H295R cells left untreated (basal) or treated for 24h with mitotane (25μM) was processed for microarray analysis. Enrichment analysis for the categories GO and heat map from microarray data with the most highly up-regulated (red) and down-regulated (blue) genes involved in the cholesterol biosynthesis pathway. **F-G**, **I-J**, **L-M**) mRNA expression of SREBP1 (**F-G**), INSIG1 (**I-J**) and ABCG1 (**L-M**) in H295R cells. The mRNA was extracted and analyzed by QPCR from cells left untreated (0) or treated for 24 h with Mitotane (10-25-40 μM) (**F-I-L**) and from cells untreated (0) or treated for different weeks (2 or 3 weeks, w) with Mitotane (10μM) (**G-J-M**). Each sample was normalized to 18S rRNA content. Final results are expressed as n-fold differences of gene expression relative to calibrator. Data represent the mean ±SD of values from at least three separate RNA samples (*p < 0.05, ***p< 0.001 versus calibrator). (**H, K, N**) Survival time in ACC patients according to the expression of SREBP1 (**H**), INSIG1 (**K**) and ABCG1 (**N**) genes. Statistical significance was calculated using t-test (**A, B, C, H, K, N**) or one-way analysis of variance followed by a Tukey post-hoc multiple comparison test (**D, F, G, I, J, L, M**), P < 0.05 was considered significant.

FIGURE 2. Simvastatin reduces H295R cell growth, in vitro and in vivo. A. H295R cells were left untreated (0) or treated with increasing doses (2.5, 5, 10 μM) of simvastatin for 24 and 48 h. **B**) H295R cells were left untreated (0) or treated with increasing doses (2.5; 5; 10 μM) of simvastatin with or without mevalonate (200 μM) for 48h. **A** and **B**) Cell viability was evaluated by MTT assay (*p< 0.05, ***p<0.001 *vs* 0). **C**) Representative image of colony formation assay performed on H295R cells (1000 cells/well) plated for 2 weeks in the presence of simvastatin (2.5, 5, 10 μM). **D**) H295R cells were plated on low-attachment plates and then left untreated (0) or treated with Simvastatin (2,5, 5 and 10 μM), tumor-spheres formation efficiency (TSFE) was evaluated 5 days later (*p<0.05 *vs* untreated cells). **E**) H295R cells were injected subcutaneously in the flank region of nude mice and the resulting tumors were grown to an average of 200 mm^3 21 days after inoculation and then treated with vehicle (n= 8) or simvastatin (n= 7) (4mg/kg/day) for 24 days. Values represent the mean ±SE of measured tumor volume over time (*p<0.05 versus control). **F**) Representative tumors and final tumor weights, values are mean ±SEM, (*p<0.05 vs vehicle). **G**) Ki67 immunohistochemistry and H&E staining of H295R xenografts (Magnification X 20, scale bar =25 μm). Statistical significance was calculated using t-test (**F**) or one-way analysis of variance followed by a Tukey post-hoc multiple comparison test (**A, B, D, E**), P < 0.05 was considered significant

FIGURE 3. Simvastatin decreases cholesterol and aromatase content in ACC. A) H295R cells were left untreated (0) or treated for 48h with simvastatin (2.5, 5, 10 μM) in growth medium containing 10% lipoprotein-free serum. Cholesterol was extracted and measured by colorimetric

assay (*p< 0.05 vs untreated cells). **B, bar graph**) Cholesterol content in H295R xenografts samples (*p< 0.05 vs vehicle) (n=8 vehicle; n=7 Simvastatin). **B, photograph**) Frozen sections of H295R xenografts from vehicle- or simvastatin-treated mice were used for lipids droplets staining by Oil Red O (Magnification X40, scale bar 12,5µm). **C**) H295R cells were treated for 48h with the indicated doses of simvastatin added to 5% DCC-FBS and estradiol (E2) release in the culture medium was measured by ELISA. Values represent the mean ±SE (*p< 0.05 vs untreated cells). **D-F**) H295R cells untreated (0) or treated for 24h with simvastatin (2.5, 5, 10 µM) were analyzed for CYP19 gene expression normalized to 18S rRNA by real-time PCR (**D**), and for SF-1 (**E**) or Aromatase (Arom) (**F**) protein content by WB. GAPDH was used as a loading control. Blots are from 1 representative experiment out of at least 3 performed. **G**) CYP19 expression in H295R xenografts samples from vehicle- or simvastatin-treated mice by real-time PCR (n=8 vehicle; n=7 Simvastatin). **H**) Immunohistochemical staining of Aromatase in untreated or simvastatin-treated H295R xenograft samples (Magnification X 20, scale bar =25 µM). Statistical significance was calculated using t-test (**B, G**) or one-way analysis of variance followed by a Tukey post-hoc multiple comparison test (**A, C, D**). P < 0.05 was considered significant.

FIGURE 4. Simvastatin reduces nuclear and mitochondrial ERα activity. A and **C**) WB analysis of ERα (**A**) and Cyclin E (**C**) was performed on equal amounts of total protein extracts from H295R cells left untreated (0) or treated with Simvastatin (2,5, 5 and 10 µM) for 48h. GAPDH was used as a loading control. Blots are representative of three independent experiments with similar results. **B and D**) Immunofluorescence analysis of ERα expression (**B**) and immunohistochemical staining of Cyclin E (**D**) on H295R xenograft tumor samples obtained from vehicle- or simvastatin-treated mice (Magnification X 20, scale bar=25 µM). **E and F**) H295R cells untreated (0) or treated with simvastatin (5 µM) were used for mitochondrial protein extraction. ERα (**E**) and OXPHOS (**F**) protein expression was analyzed by WB. GAPDH was used as a loading control. Blots are representative of three independent experiments with similar results. **G** and **H**) Immunostaining (**G**) and activity (**H**) of COX IV was evaluated on H295R xenograft samples obtained from vehicle- or simvastatin-treated mice (Magnification X 20, scale bar = 25µm).

FIGURE 5. Simvastatin reduces mitochondrial functions. A-F) Mitochondrial respiration described as OCR (oxygen consumption rate) levels was detected in H295R cells left untreated or treated with Simvastatin (2.5, 5, 10 µM) for 16h by Seahorse XFe96 analyzer. **A**) The linear graph shows time course measurements but with three different injections to evaluate the OCR 1- after the oligomycin injection, 2- after the injection of carbonyl cyanide-(trifuoromethoxy)phenylhydrazone (FCCP), 3- after the injection of rotenone/antimycin. **B-F**) The histograms are derived from the obtained measurements: (**B**) basal respiration, (**C**) maximal respiration, (**D**) proton leak, (**E**) ATP turnover and (**F**) spare capacity (*p<0.05, ***p< 0.001 simvastatin *vs* untreated cells). **G**) Mitochondrial extracts from H295R cells treated for 48h were analyzed for TOM20 protein expression by WB. **H**) TOM20 protein expression was evaluated by immunohistochemistry on H295R xenograft samples obtained from vehicle- or simvastatin-treated mice (Magnification X 20, scale bar = 25µm).

FIGURE 6. In vitro and in vivo activation of apoptosis by simvastatin in ACC. A) Cells were left untreated (0) or treated with simvastatin (2.5, 5, 10 µM) for 48h. WB analyses of Bak and PARP-1 were performed on equal amounts of total protein extracts. GAPDH was used as a loading

control. Blots are representative of three independent experiments with similar results. **B**) TUNEL assay was performed on cells treated as described in **A**). DAPI was used as nuclear counterstain. Fluorescent signal was observed under a fluorescent microscope. Images are from a representative experiment. **C)**. TUNEL staining was performed on frozen sections of H295R xenograft samples obtained from vehicle- or simvastatin-treated mice (scale bar 25 µm). **D)** WB analyses for p-cJun, c-Jun, pERK1/2, ERK2, PARP-1, were performed on total protein extracted from cells treated for 48h with simvastatin (5 µM), mevalonate (100 µM), or their combination. **E**) WB analyses for p-cJun, Jun, pERK1/2, ERK2, PARP-1, were performed on total protein extracted from cells treated for 48 h with simvastatin (5 µM) alone or combined with PD98059 (10 µM), SP600125 (10 µM), SB203580 (10 µM). GAPDH was used as a loading control.

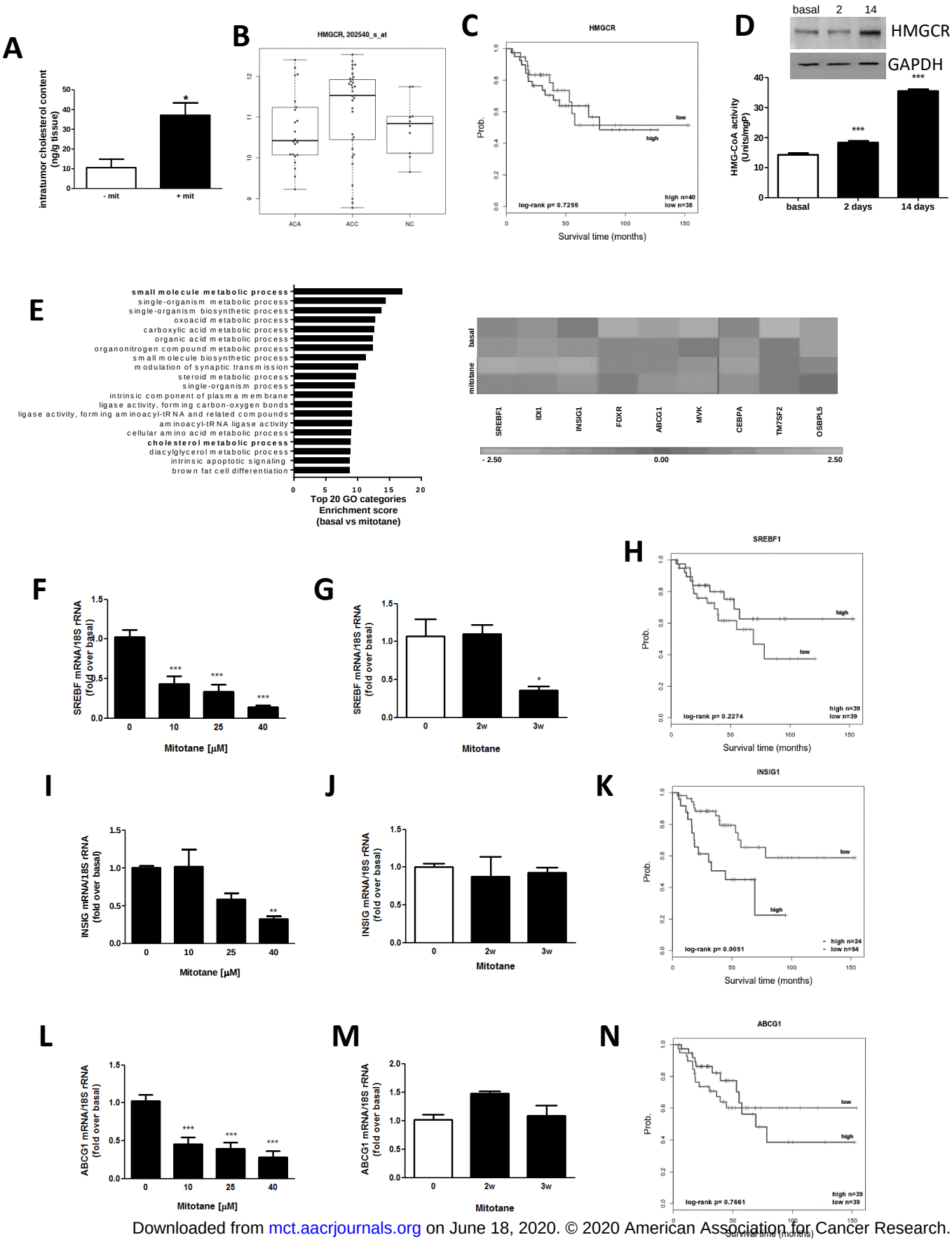

Fig. 2

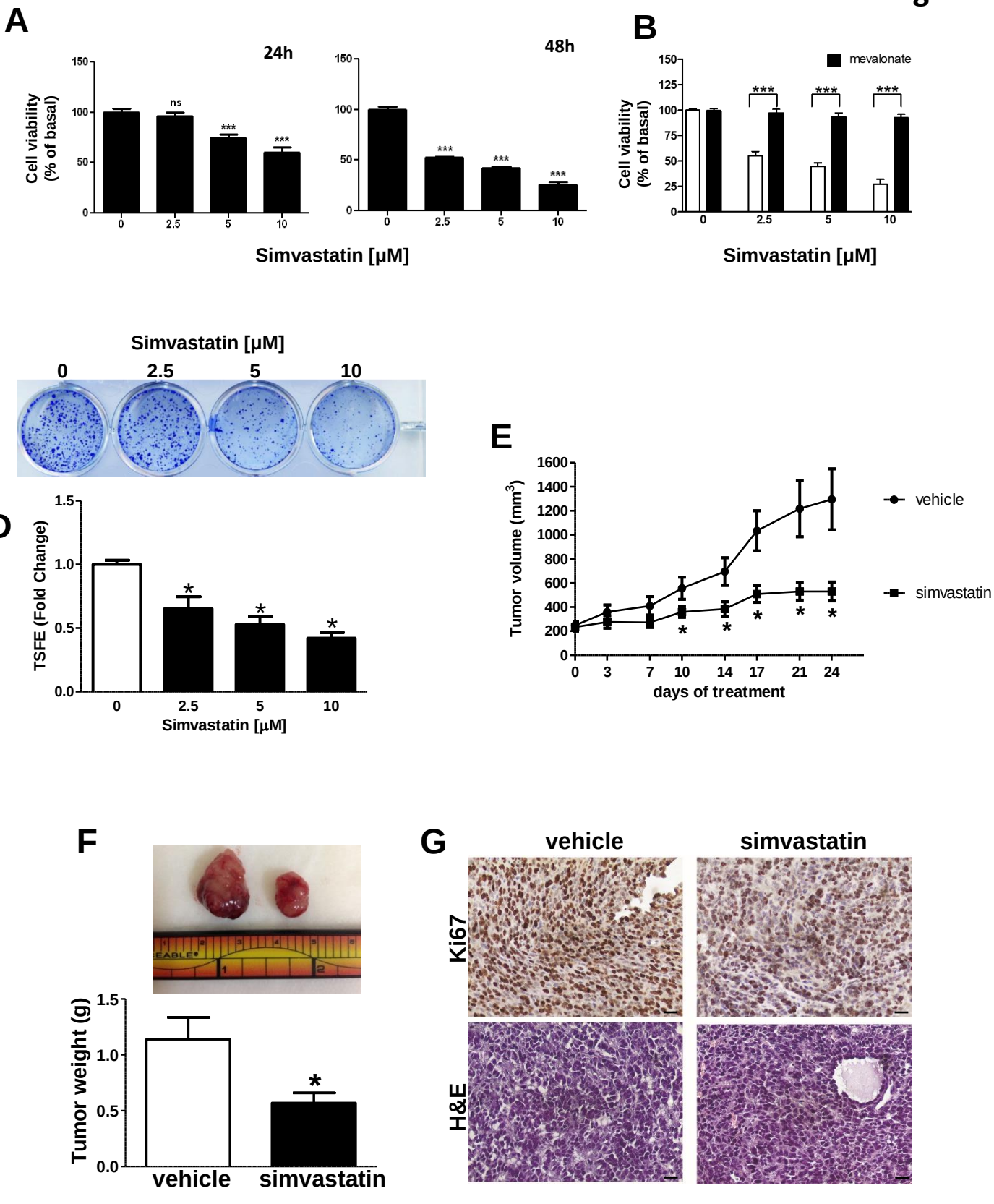

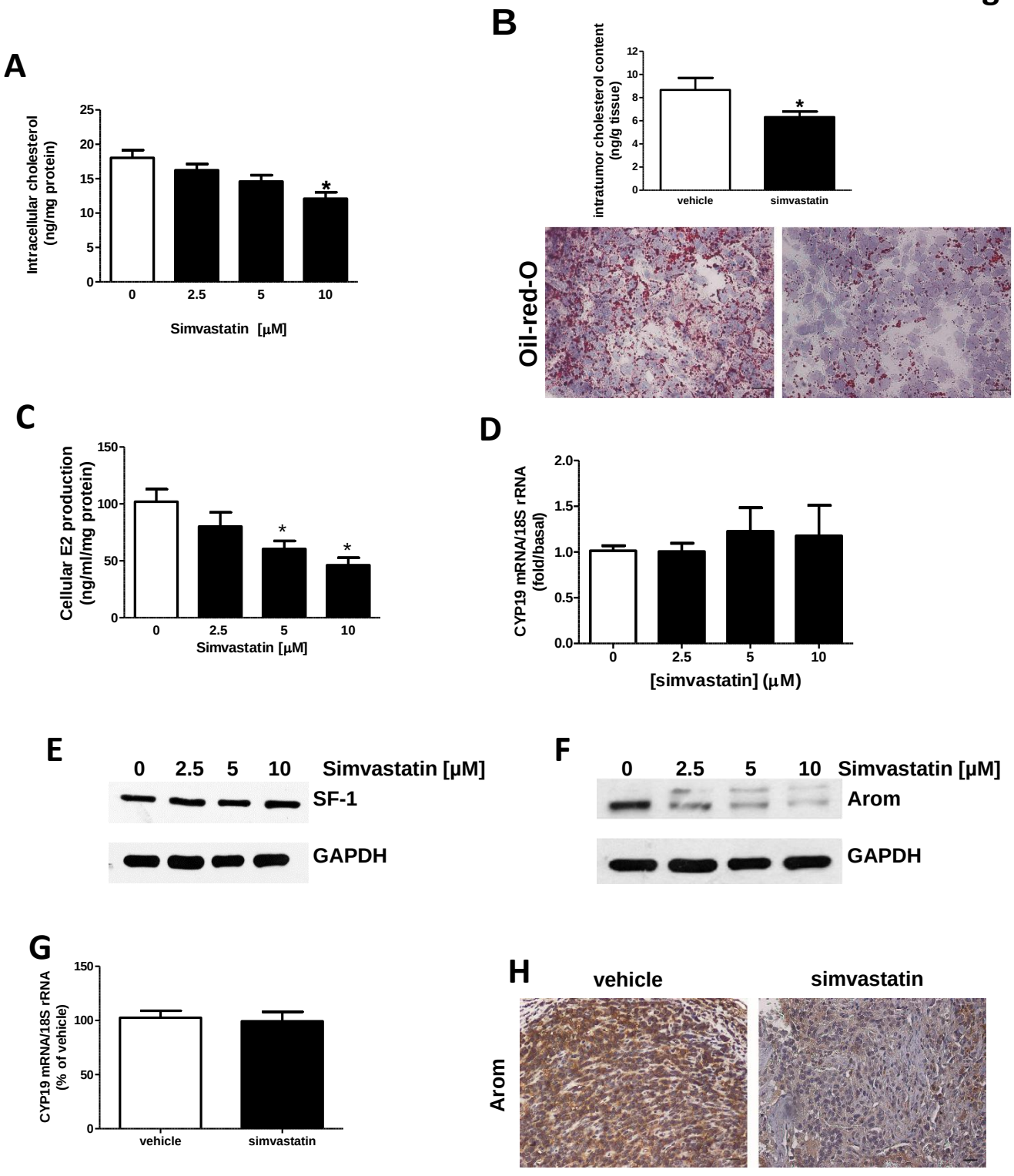

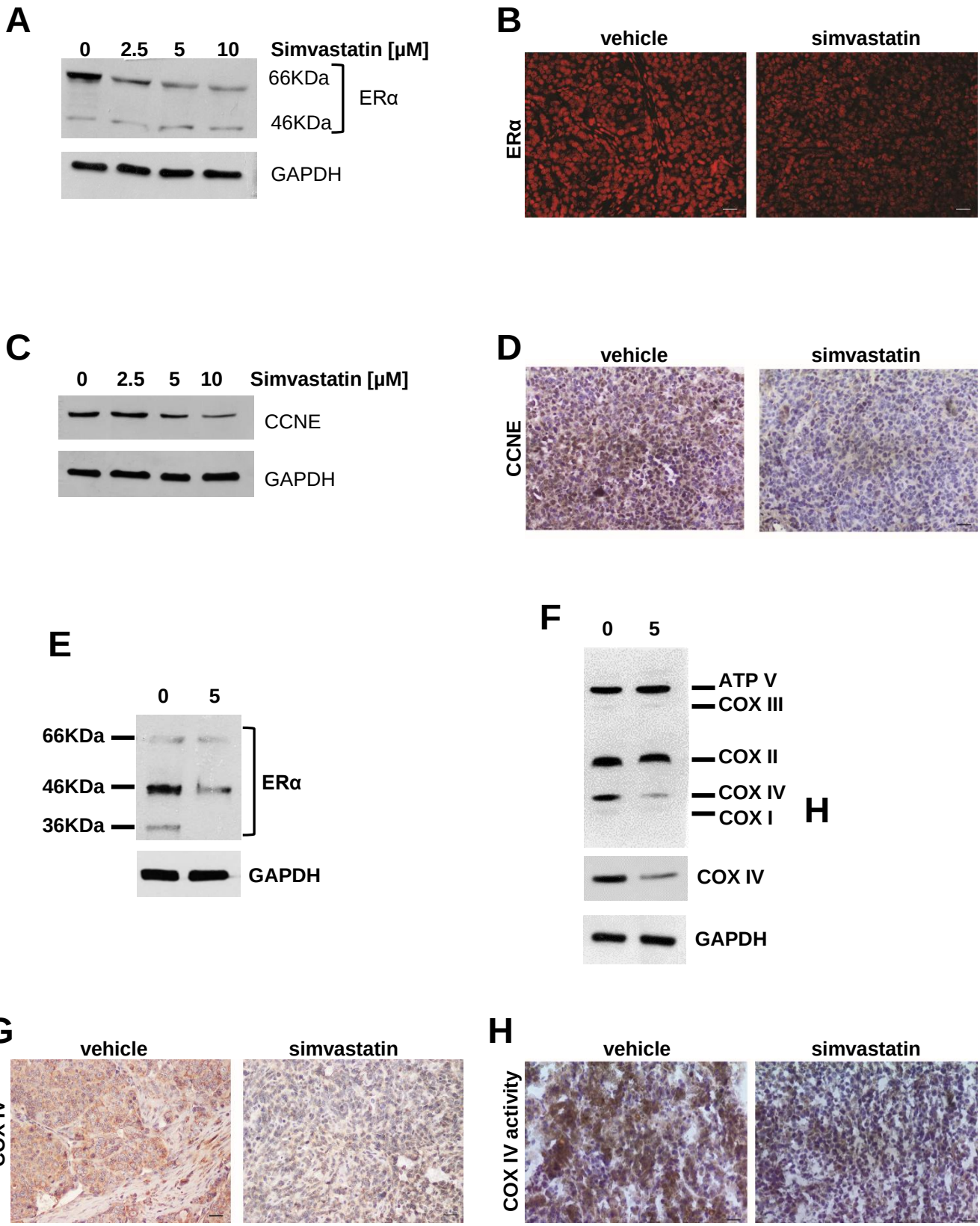

Fig. 5

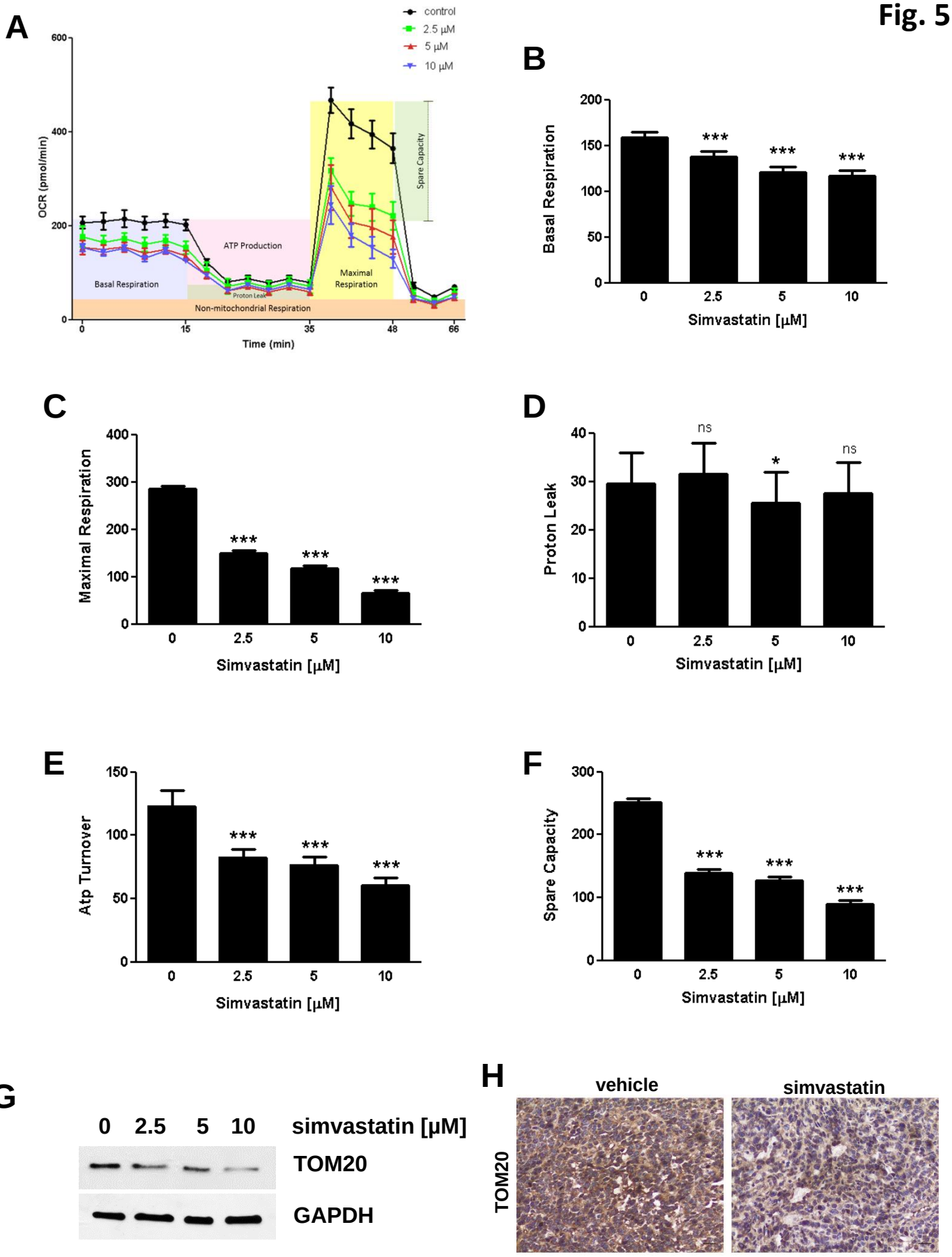

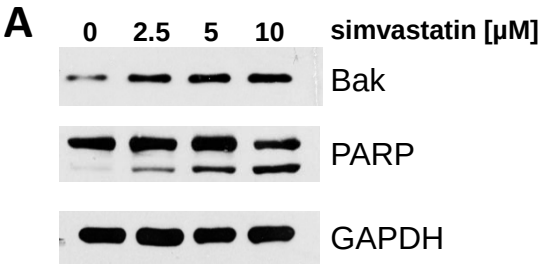

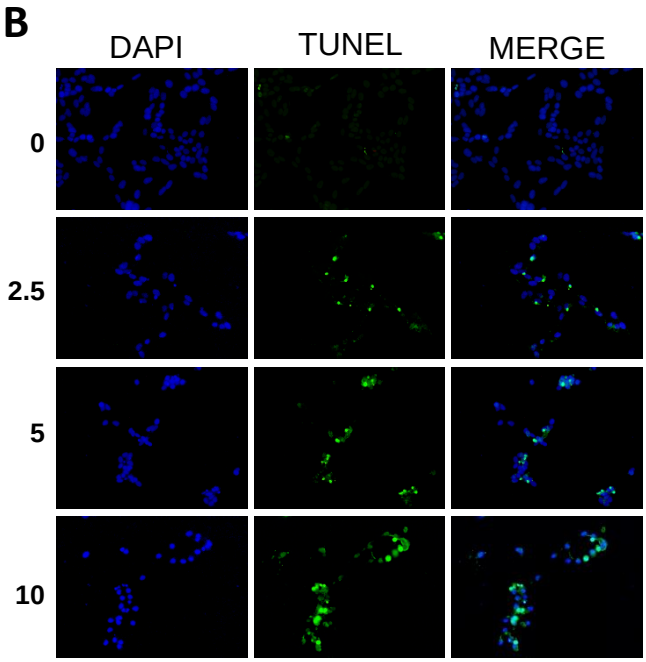

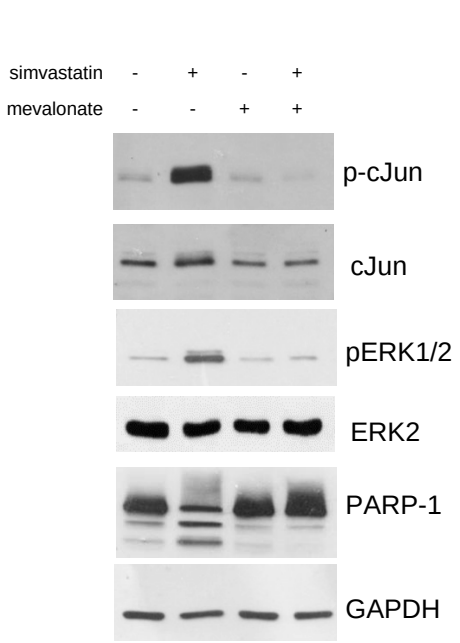

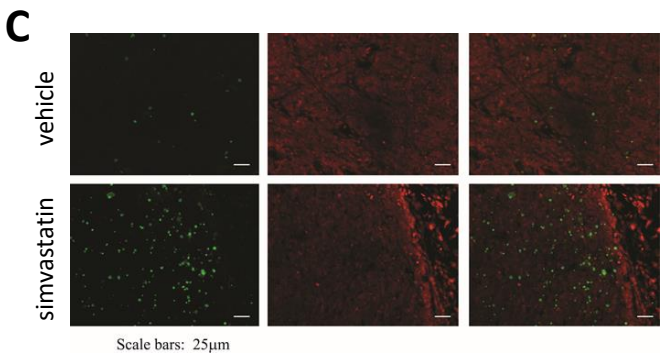

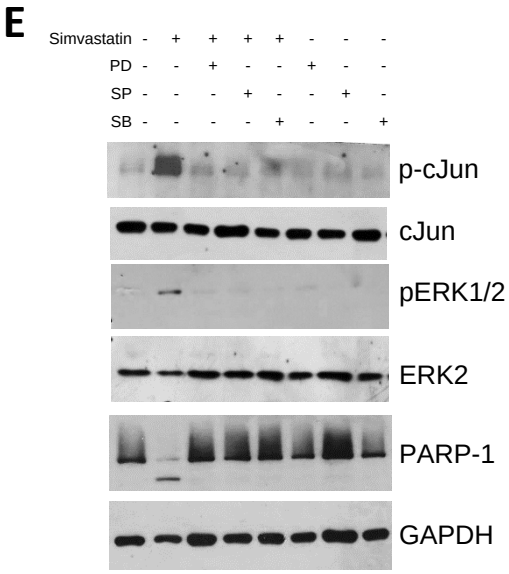

AACR American Association for Cancer Research

Molecular Cancer Therapeutics

Statins reduce intratumor cholesterol affecting adrenocortical cancer growth

Francesca Trotta, Paola Avena, Adele Chimento, et al.

Mol Cancer Ther Published OnlineFirst June 16, 2020.